Utilizing Air-Turborocket and Rocket Propulsion for a Single-Stage-to-Orbit Vehicle

Roger A. Lepsch Jr.,* Douglas O. Stanley,† Christopher I. Cruz,† and Shelby J. Morris Jr.‡
NASA Langley Research Center, Hampton, Virginia 23665

A horizontal-takeoff, single-stage-to-orbit launch vehicle was designed that utilized a combination of air-turborocket and rocket propulsion systems. Weight reductions were taken on vehicle systems to simulate an advanced technology level. Both air-turborocket and rocket thrust were varied to optimize vehicle weight. For the reference vehicle, weight, propulsion, geometry, and performance characteristics are summarized. A detailed ascent trajectory analysis including trim of the reference vehicle was conducted. Finally, the sensitivity of vehicle weight-to-weight reduction assumptions is presented.

Nomenclature

A_c = inlet frontal projected area (capture area), ft^2
a_x = axial acceleration, g
a_z = normal acceleration, g
C_t = installed specific thrust coefficient ($F_n/q_\infty A_c$)
F_n = installed net thrust (thrust-inlet drag), lb
g = gravitational acceleration, 32.2 ft/s^2
I_{sp} = engine specific impulse (thrust/flow rate), s
M = Mach number
q_∞ = freestream dynamic pressure, psf
RCS = Reaction Control System
T/W = thrust-to-weight ratio
T/W_i = initial vehicle thrust-to-weight ratio
T/W_{rs} = vehicle thrust-to-weight ratio at rocket start
α = angle of attack, deg
ΔV = change in relative velocity, ft/s^2

Introduction

CURRENTLY, there is an effort to define options for the nation's next manned space transportation system. One option, the Advanced Manned Launch System (AMLS),[1,2] is a completely new, fully reusable, operationally efficient system. A wide variety of vehicle types and propulsion systems have been examined as a part of this study. If current projections to extend the Space Shuttle's operational life beyond 2010 hold true, advanced enabling technologies currently under study for the AMLS and National Aero-Space Plane programs may be developed, and the single-stage-to-orbit (SSTO) concept may become a realistic option.

Because of the uncertainty of the initial operating date of any new launch vehicle system, SSTO vehicles are being considered as a part of the AMLS study. Single-stage vehicles simplify launch operations compared with multistage vehicles and therefore have the potential to reduce launch costs. However, they are inherently more sensitive to weights and performance assumptions, making them riskier designs to develop. The purpose of this paper is to develop and determine through analysis the characteristics of a candidate SSTO vehicle that utilizes rocket and air-turborocket (ATR) propulsion with advanced technologies to satisfy a space station logistics mission. The vehicle presented in this paper is similar to the British Aerospace HOTOL concept that takes off horizontally with the support of a trolley, utilizes airbreathing engines in the first phase of flight, and makes a transition to rocket engines at high supersonic Mach numbers.[3] These features may give the vehicle advantages over vehicles employing only rocket propulsion or vehicles that utilize airbreathing propulsion to high hypersonic Mach numbers. The airbreathing propulsion system gives the vehicle capabilities that an all-rocket-powered vehicle does not have, such as self-ferry, offset launch, and landing go-around. The transition to rocket at high supersonic Mach number instead of high hypersonic Mach number avoids the need for a supersonic combustion propulsion system (scramjet) and avoids the complexities and weight penalties associated with actively cooling airframe and engine components in the severe thermal environment that would be encountered at high Mach number and high dynamic pressure.

Trade studies will be presented that vary the vehicle thrust-to-weight ratio at initial conditions and after transition to the rocket phase to optimize total vehicle dry and gross weights (where dry weight is defined as the weight of the vehicle without propellant, other fluids, payload, or crew). Estimated vehicle weight characteristics, sensitivities, engine characteristics, geometry, performance, structures, and subsystems will be summarized.

Propulsion Systems

Air-Turborocket

The airbreathing propulsion system chosen for this study is the air-turborocket (ATR), a schematic of which is shown in Fig. 1. The ATR is characterized by a fan driven by a turbine that is independent of the fan airflow. The working fluid of the turbine is supplied by a rocket gas generator operating fuel rich. The compressed air from the fan is ducted around the turbine and into an afterburner where additional fuel is added and combustion occurs. The ATR was chosen because it has supersonic cruise efficiency equal to that of a ramjet, high

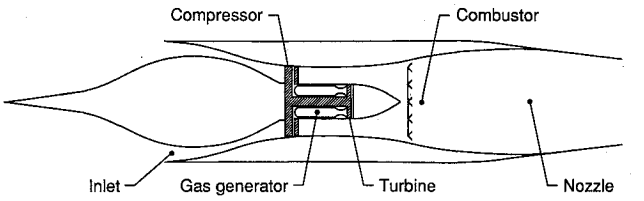

Fig. 1 Schematic of typical air-turborocket engine.

Presented as Paper 90-0295 at the AIAA 28th Aerospace Sciences Meeting, Reno, NV, Jan. 8-11, 1990; received Feb. 11, 1990; revision received Feb. 13, 1991; accepted for publication Feb. 14, 1991.

*Aerospace Engineer, Space Systems Division.
†Aerospace Engineer, Space Systems Division. Member AIAA.
‡Aerospace Engineer, Advanced Vehicles Division. Member AIAA.

Table 1 Engine specifications of ATR

Airflow size (at sea level static)	1847 lb/s
Fan pressure ratio	2.0
Turbine inlet temperature	3500°R
Specific thrust (at sea level static)	170 lb/lb air
Sea level static thrust	314,782 lb
Inlet capture area, A_c	81.0 ft^2
Operational Mach number range	0–6.2

takeoff thrust, and relatively high operational Mach number. A complete cycle description of this engine is contained in Ref. 4.

Table 1 lists the engine specifications assumed for the ATR. These specifications were determined by a computer code employing one-dimensional cycle analysis and assuming chemical equilibrium. The fuel and oxidizer utilized are liquid hydrogen (LH_2) and liquid oxygen (LOX), respectively. High engine performance was achieved by extending combustion temperatures beyond the limits of near-term materials. Therefore, the data presented here should be considered optimistic in that they reflect the application of far-term materials.

Installed specific thrust coefficient (C_t) and specific impulse (I_{sp}) are given over a range of dynamic pressures (q_∞) as a function of Mach number (M) in Figs. 2 and 3, respectively. A precompression effect equivalent to a 5-deg wedge in the freestream has been included. Because the parameters are for the installed engine, the inlet ram and spillage drag has been taken into account in the thrust calculation. The maximum operational Mach number of the ATR is constrained by the maximum temperature limits of the fan. For this study, the materials utilized in the fan are assumed to allow operation up to a Mach number of 6. It should also be noted that at low subsonic speeds ($M \leq 0.3$), the airflow demanded by the engine requires that an auxiliary inlet be opened.

Rocket

The rocket propulsion system chosen for this study is based on the Space Shuttle main engine (SSME) with some modifications. Because operation of the rocket system occurs only at high altitudes, the standard SSME nozzle was replaced with a 150:1 expansion ratio nozzle to improve specific impulse. Also, the nozzle throat diameter was increased slightly to increase thrust.

With a higher expansion ratio and a larger throat, the engine is estimated to produce a maximum thrust of 564,000 lb and a specific impulse of 462.5 s, at vacuum conditions. The SSME utilizes LOX and LH_2 propellants in a ratio of 6:1 by weight.

For this study, both the ATR and rocket engines were scaled to meet vehicle thrust requirements. The point designs described were used to obtain parametric performance data. Propellant flow rates and thrust were assumed to vary directly with exit area, while nondimensional coefficients and thrust-to-weight ratio were assumed to remain constant.

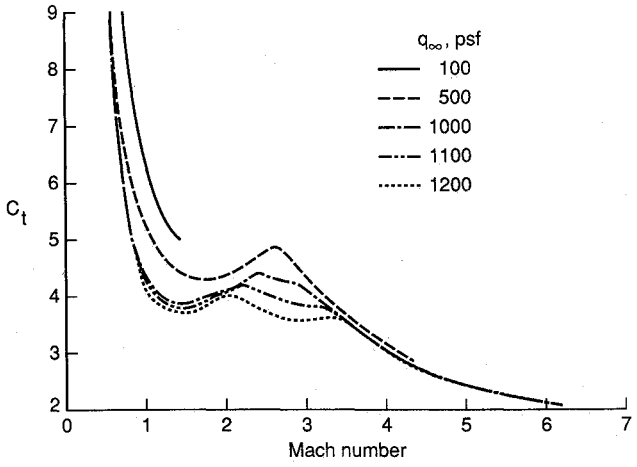

Fig. 2 ATR installed specific thrust coefficient.

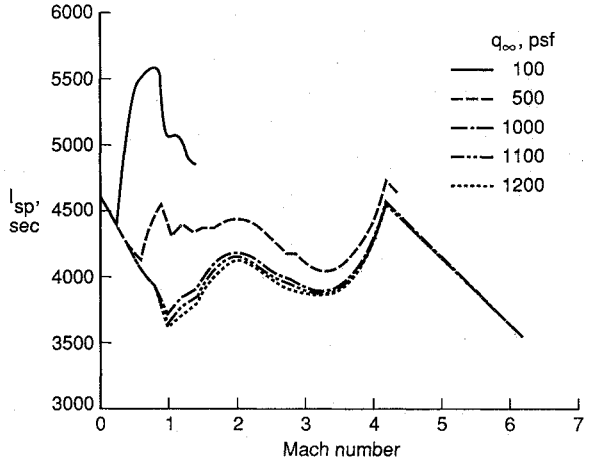

Fig. 3 ATR installed specific impulse.

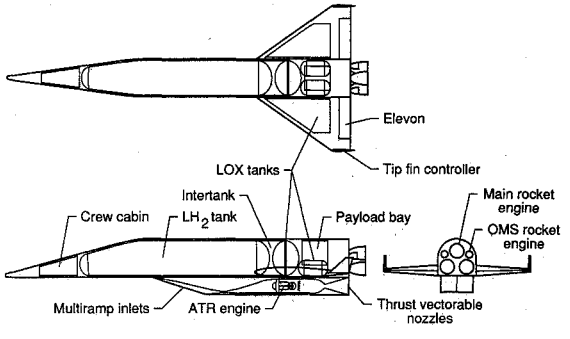

Fig. 4 Reference vehicle configuration.

Vehicle Configuration

The vehicle concept developed for this study is a horizontal-takeoff, horizontal-landing configuration that utilizes an unpowered trolley for launch. The trolley supports the wings and fuselage during the takeoff run; hence, the landing gear need only be sized to withstand the landing loads of the empty return vehicle. Although abort cases were not specifically studied in this paper, it is assumed that propellants would be dumped or burned during an abort so that maximum landing loads would not be exceeded.

The vehicle is fully reusable for operational simplicity. All propulsion systems on the vehicle utilize LH_2 and LOX propellants to further improve operations by reducing the number of fluids required. In addition, the vehicle's landing gear, surface controls, and engine gimbals are electrically actuated to eliminate hydraulic systems.

A vehicle configuration is pictured in Fig. 4 (trolley not shown). The ATR propulsion system is located underneath the body and is installed in a twin engine configuration. The inlets are of a two-dimensional, multiramp design. These inlets may require complex variable geometry to improve vehicle aerodynamics and prevent airflow to the engines when not in operation. The nozzles can be vectored to assist in vehicle pitch control. The vehicle employs control configuring to provide stability augmentation in both pitch and yaw.[5,6] Control configuring reduces the size of the tip fins because they are sized for control, not stability, and allows the vehicle to fly with a more aft center-of-gravity location. Insulated tanks containing LOX are located in the wings to provide wing load relief during flight and reduce fuselage propellant volume requirements.[7] Wing tanks require more insulation than fuselage tanks because of their greater surface-area-to-volume ratio

Table 2 Mission requirements and guidelines

Launch site	KSC
Target orbit	262 nmi circular
Orbit inclination	28.5 deg
Payload weight	20,000 lb
OMS ΔV	1350 ft/s
RCS ΔV	150 ft/s
Payload dimensions	15 × 16 ft cylinder
Number of crew	10
Mission duration	3 days

and their design is more complex, which increases their weight. However, these disadvantages are offset by the structural weight savings resulting from lower wing loads and a reduction in fuselage size.

The structural arrangement and material requirements for the vehicle are as follows. The forward portion of the fuselage contains the crew cabin, integral LH_2 tank, intertank, and integral LOX tank. The aft portion contains the payload bay, rocket engine bay, and two nonintegral LOX tanks. The aft portion of the fuselage, the wing, and the ATR cowling are hot structures and hence do not require a thermal protection system. This hot structure design requires internal insulation to protect the contents from reaching excessive temperatures. Extensive use of high temperature, high specific strength materials will be required for the hot structures. Titanium-aluminide metal matrix composites appear to be promising, with temperature limits potentially up to 1800°F[8] and specific strength considerably better than high temperature superalloys. Advanced carbon-carbon composites will be needed in higher temperature areas like the nose and wing leading edges and the interior of the inlets. Propellant tanks will need to be lightweight and made from materials that can endure repeated exposure to cryogenic temperatures. Aluminum-lithium alloys and reinforced thermoplastic composites are candidate tank materials that promise significant weight reductions. However, these are not high temperature materials and will require thermal protection. Insulated panels of titanium-aluminide or some other high temperature material will be necessary to protect the tanks.

Mission, Guidelines, and Trajectory

The mission requirements and guidelines used in this study are summarized in Table 2. These guidelines satisfy the space station resupply mission as defined by the AMLS study. A 20,000-lb payload delivery and return capability is required. The mission profile includes ascent to a 262-n.mi. circular orbit, a 3-day on-orbit stay, deorbit, descent, and an unpowered landing.

A similar flight sequence and similar constraints are employed in all the trajectories performed in this study. The vehicle and trolley begin the takeoff run and accelerate along the runway under the power of the vehicle's ATR engines. At a speed of approximately Mach 0.4, the trolley allows the vehicle to rotate to an angle of attack (α) of 20 deg, and the vehicle separates and takes off. At takeoff, the vehicle is limited to a normal acceleration (a_z) of 1.2 g. This low value was chosen to minimize wing design loads and therefore wing weight; however, some form of gust alleviation may be required. To achieve efficient operation of the ATR and reduce vehicle drag, α is reduced to a low value as the vehicle accelerates through the transonic region. Once beyond the transonic speed range, the vehicle continues accelerating until a dynamic pressure (q_∞) of 1200 psf is reached. The vehicle then modulates α to hold this q_∞ constraint to insure an efficient accelerating climb in a relatively benign heating environment. Just before the limit of ATR operation is reached, at Mach 6, the vehicle performs a pull-up maneuver to achieve a high flight-path angle to begin the rocket-powered phase. When the pull-up has been completed, the ATR engines are shut down , and the rocket engines are started. The vehicle then continues on a low-heat-rate, low-dynamic-pressure ascent. During this segment of the flight, the axial acceleration (a_x) is limited to 3 g, as with the Space Shuttle, by throttling back the rocket engines. The rocket engines shut down upon insertion into an optimal elliptical orbit. An orbital maneuvering system (OMS) is used to circularize the orbit at the required altitude.

Throughout the trajectory, vehicle flight control deflections were constrained to realistic values. The elevons were allowed to deflect up or down a maximum of 25 deg. The rocket engines were allowed to gimbal up to 10 deg in any direction, and the ATR nozzles were allowed to deflect from 0 to 15 deg down.

Analysis

The aerodynamic analysis was performed using the Aerodynamic Preliminary Analysis System (APAS).[9] The APAS is capable of analyzing three-dimensional configurations having multiple surfaces of arbitrary planform and bodies of noncircular contour. Analysis methods are based on potential theory at subsonic and supersonic speeds and impact-type finite element solutions at hypersonic speeds.

The APAS was used to provide the vehicle lift, drag, and moment information for the trajectory analysis. A combination of elevon deflection and thrust vectoring was used for pitch control. The location of the ATR engines significantly below the center of gravity of the vehicle necessitated that the effect of its thrust on the trim characteristics of the vehicle be included in the analysis. No attempt was made to account for the effects of inlet spillage lift on the trim characteristics of the vehicle.

The three-degrees-of-freedom version of the Program to Optimize Simulated Trajectories (POST) was utilized to perform the trajectory analysis.[10] The POST is a generalized, event-oriented trajectory program that can be used to analyze ascent, on-orbit, and entry trajectories. Any calculated variable in POST can be optimized while subject to a combination of both equality and inequality constraints. Only ascent trajectories were analyzed.

The weights, balance, and sizing analysis was performed using the Configuration Sizing (CONSIZ) program. The CONSIZ program is capable of determining the mass properties and size of a variety of launch vehicle types. Weight estimating relationships corresponding to the vehicle components are input to the program and can be easily modified to incorporate updates when necessary. Sizing is performed by scaling the geometry of a point design vehicle photographically until vehicle weights and propellant volumes satisfy mass ratio and oxidizer-to-fuel ratio requirements obtained from a trajectory analysis.

The vehicle weights were predicted using statistically developed, historically based weight-estimating relationships (WERs). These WERs were either obtained from sources on weight estimation methods[11–13] or were developed in-house using available weights data on existing aircraft and spacecraft. Space Shuttle weight reports[14,15] were used as a primary source of information for many vehicle systems. Weight factors were applied to these WERs to account for advanced technology. A weight factor for a vehicle component is simply the weight of that component after a given technology has been applied, divided by the original weight. The weight factors applied in this study were chosen to define a far-term technology level and are meant to illustrate what vehicle characteristics result if these values are assumed. Given the structural materials applied to the study vehicle, it is known that large weight reductions will be possible with respect to Space Shuttle technology. For instance, based on a comparison of the predicted specific strength of titanium-aluminide metal matrix composites (1.2–1.6 × 10^6 in)[16] with the specific strength of conventional aluminum (0.6–0.8 × 10^6 in), a weight savings of roughly 50% is possible. However, to accurately assess the impact of this and other advancements in technology, a more detailed analysis is required.

To apply the weight factors, the vehicle weights were grouped into four categories: structures (including landing gear), subsystems, ATR propulsion, and rocket propulsion. Vehicle structures, ATR propulsion, and rocket propulsion were all reduced by 50% and vehicle subsystems were reduced by 30%. After weight reductions, the thrust-to-weight ratio (T/W) of the installed ATR at sea level (including inlet and nozzle weight) is 13.3, and the T/W of the SSME with an expansion ratio of 150:1 is 124 at vacuum conditions.

Results

Vehicle Thrust-to-Weight Ratio Trades

For this study the vehicle T/W at initial conditions (T/W_i) and at rocket startup (T/W_{rs}) was optimized with respect to dry and gross weight. In the optimization of T/W_{rs}, the rocket phase was treated as independent of the airbreather portion of the flight. This was allowable because the transition point (Mach 6 at a q_∞ of 750 psf) was held constant throughout this study, and hence the initial conditions of the rocket portion of the ascent trajectory remain relatively constant. Once an optimum T/W_{rs} was determined, this value was held constant throughout the T/W_i trade.

Rocket-Powered Mode

To determine the effect of varying T/W_{rs} on vehicle weights, the performance of several cases was evaluated. The cases evaluated for this trade had T/W_{rs} values of 0.9, 1.0, 1.1, 1.2, 1.3, and 1.4. All of these cases were evaluated with T/W_i equal to 0.8. The most important performance parameters resulting from the trajectory analysis of each case are the oxidizer-to-fuel ratio (O/F) and the mass ratio (i.e., the vehicle gross weight divided by the burnout weight).

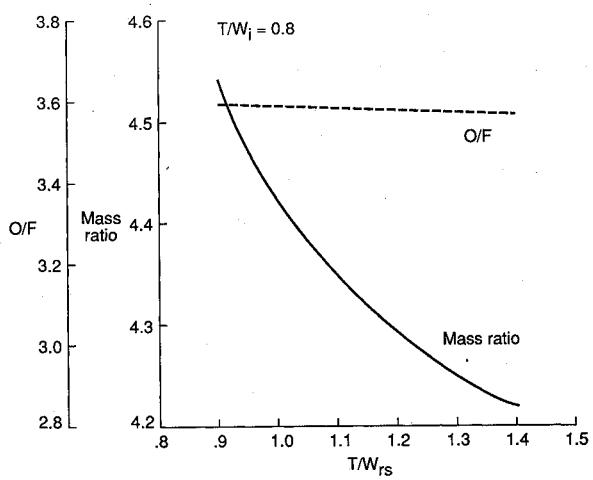

Fig. 5 Effect of T/W_{rs} on performance parameters.

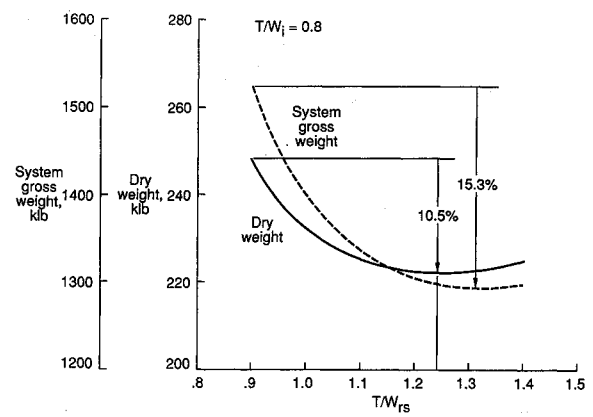

Fig. 6 Effect of T/W_{rs} on vehicle sizing.

Figure 5 illustrates the influence of varying T/W_{rs} on these performance parameters. As indicated by the lower mass ratios, performance improves as T/W_{rs} increases because less propellant is consumed. The overall O/F decreases slightly as T/W_{rs} increases over the range evaluated. This is due to the decrease in LOX consumption in the rocket phase and the fact that LH_2 consumption in the ATR phase remains unchanged. A lower mass ratio is favorable for vehicle sizing; however, the influence of the added propulsion system weight must be accounted for to assess the impact on vehicle sizing. Hence, the vehicle was resized for each of the cases examined. The effect of varying T/W_{rs} on vehicle sizing is shown in Fig. 6. The T/W_{rs} value that results in the lowest vehicle dry weight is approximately 1.25. A T/W_{rs} value of approximately 1.3 is shown to provide the lowest system gross weight.

Air-Turborocket-Powered Mode

To determine the effect of varying T/W_i on vehicle weights, the performance of several cases was evaluated. The cases evaluated had T/W_i values of 0.5, 0.6, 0.7, and 0.8. All cases kept a T/W_{rs} value of 1.25, which optimized dry weight from the rocket mode T/W trade.

The effect of varying T/W_i on the altitude profile of the vehicle is shown in Fig. 7. As T/W_i decreases, the thrust-to-drag margin also decreases, and the airbreathing portion of the flight becomes progressively longer. This leads to an increase in the velocity losses associated with vehicle drag, and performance suffers. This effect is illustrated in Fig. 8 by the increase in mass ratio as T/W_i decreases. Because the vehicle spends more time in the airbreathing phase of flight when T/W_i values are lower, the amount of LH_2 consumed is greater. This results in lower values of O/F as shown in the

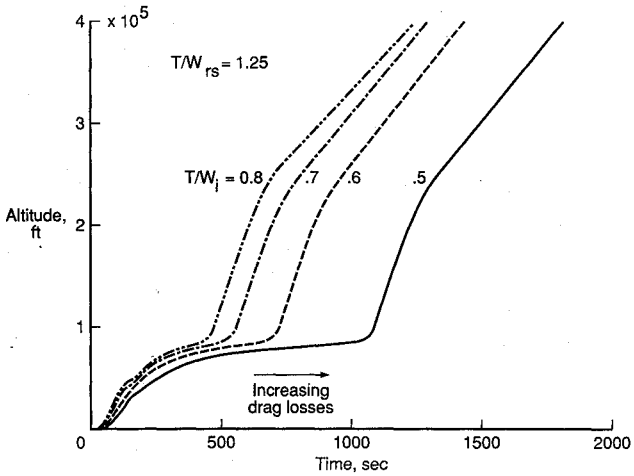

Fig. 7 Effect of T/W_i on altitude profiles.

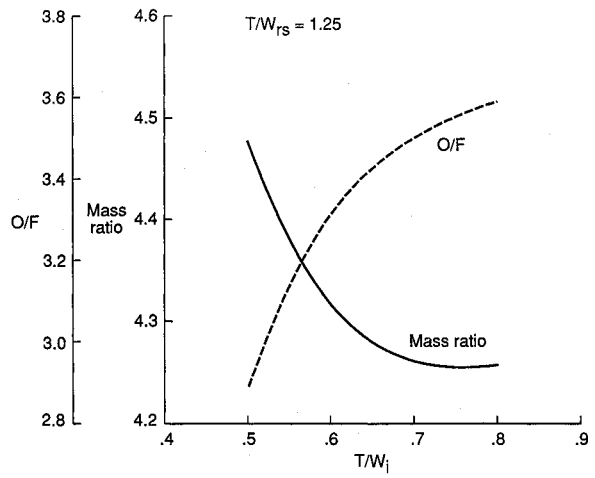

Fig. 8 Effect of T/W_i on performance parameters.

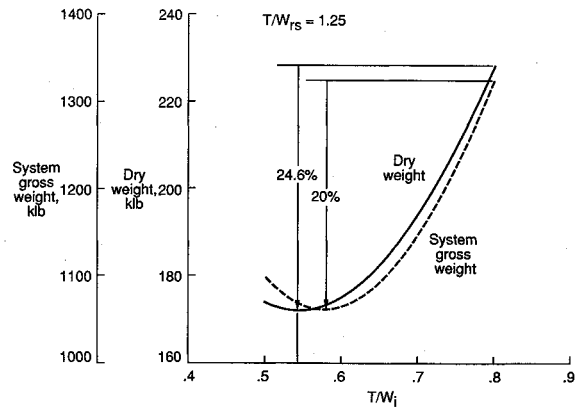

Fig. 9 Effect of T/W_i on vehicle sizing.

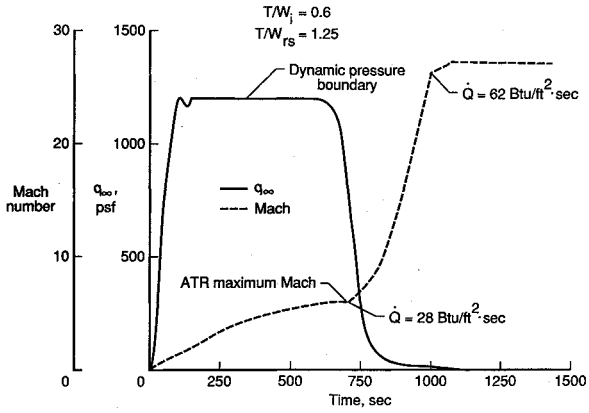

Fig. 10 Reference vehicle dynamic pressure and Mach number profiles.

figure. A lower mass ratio and a higher O/F is favorable for vehicle sizing. When LH_2 and LOX propellants are used, a higher O/F results in a higher bulk density for the propellant combination. This reduces the propellant volume requirements and, therefore, the vehicle size. At the higher T/W_i values, the mass ratio is lower, and the O/F ratio is higher. However, the influence of the added propulsion system weight (which is quite large for the ATR) must again be accounted for to accurately assess the impact on vehicle sizing. As with the rocket T/W trade, the vehicle was resized for each of the cases examined. The influence of varying T/W_i on vehicle sizing is shown in Fig. 9. The lowest total dry weight occurs for a T/W_i value of approximately 0.55, while the lowest system gross weight occurs for a T/W_i value of approximately 0.58. Lower dry weight generally indicates lower production cost for a given vehicle. Based on this trade, the lowest dry weight of the SSTO vehicle is just over 170,000 lb, with a corresponding total gross weight of 1,050,000 lb.

The sensitivity of the vehicle to both T/W_i and T/W_{rs} illustrates the necessity of optimizing vehicle weight with respect to these two parameters. This is especially true of T/W_i because of the influence of the ATR's high system weight-to-thrust ratio.

Reference Vehicle Characteristics

Analysis results are discussed for the vehicle case with T/W_i equal to 0.6 and T/W_{rs} equal to 1.25. This vehicle was chosen as the reference because it is near optimum with respect to overall dry weight.

Ascent Trajectory

The dynamic pressure and Mach number profiles for the reference vehicle are shown in Fig. 10. As shown, a dynamic

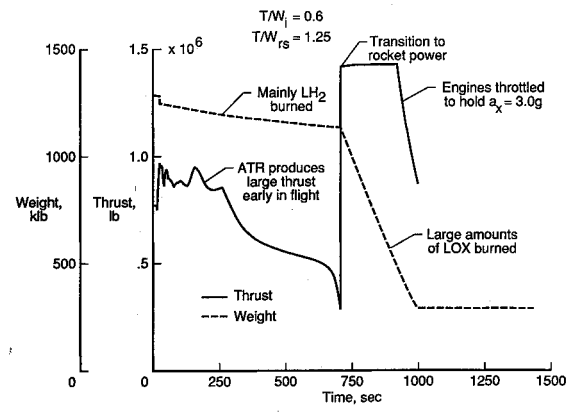

Fig. 11 Reference vehicle weight and thrust histories.

pressure boundary of 1200 psf is held for a majority of the airbreathing phase. During the pull-up maneuver described earlier and after rocket transition, the dynamic pressure falls rapidly. Also, the altitude and Mach number both increase at a much faster rate after rocket transition than during the airbreathing phase.

The POST is capable of calculating the maximum reference stagnation point heat rate, which can be used as a general indicator of the heating encountered by the vehicle. It should be noted that the vehicle remains in a relatively benign heating environment throughout the airbreathing phase. The maximum reference stagnation point heat rate for the airbreathing phase is 28 Btu/ft^2·s, which occurs at Mach 6. The maximum reference stagnation point heat rate encountered during the entire ascent was 62 Btu/ft^2·s, which occurs at vehicle burnout and should be considered typical of rocket ascents.

The thrust and weight profiles of the vehicle throughout the ascent are shown in Fig. 11. As shown in the figure, a characteristic of the ATR used in this study is that it produces large amounts of thrust early in the flight. This is an advantage in that it reduces the takeoff run and also reduces the time spent accelerating through the transonic regime where vehicle drag is high. However, at approximately 300 s the thrust begins to decrease rapidly. A decrease in ATR thrust of approximately 65% occurs as the flight time advances from 300 to 700 s. During this time, the vehicle Mach number increases from approximately 4 to 6. In this region, vehicle performance suffers because of a decreasing thrust-to-drag margin. This indicates

Table 3 Summary weight statement for reference vehicle

System	Weight, lb
Structure	74,400
Propulsion	63,250
Airbreathing	49,080
Rocket	14,170
Subsystems	20,100
Margin	17,450
Dry	175,200
Non-cargo	4,100
Cargo	20,000
Inert	199,300
Consumables	2,600
Propellant	832,100
RCS and OMS	25,900
Ascent	794,500
Reserve and residual	11,700
Gross vehicle	1,034,000
Launch assist	31,000
Gross system	1,065,000

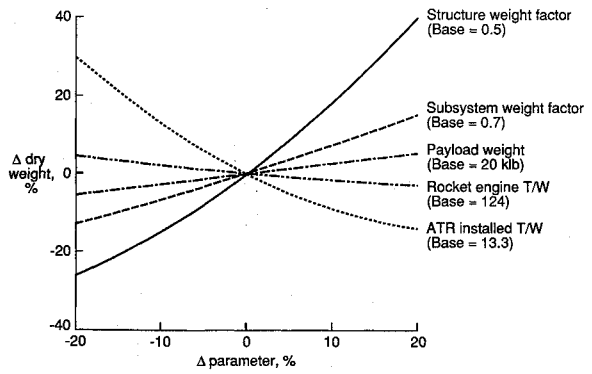

Fig. 12 Reference vehicle weight sensitivity.

that it may be beneficial to make a transition to rocket thrust earlier in the flight or to operate the propulsion systems concurrently for a time before making a transition to rocket power alone.

Figure 11 also shows that the weight of the vehicle decreases little in the ATR-powered phase because of the relatively high specific impulse where mainly LH_2 is burned. After the vehicle makes a transition to the rocket system, vehicle weight decreases much more rapidly because of the low rocket specific impulse with increased consumption of the heavier LOX propellant. Engine throttling is required near the end of the ascent so that the axial acceleration limit of 3 g is not exceeded.

Weights and Geometry

A summary weight statement of the reference vehicle is shown in Table 3. The dry weight of the vehicle is 175,200 lb, and the total gross weight, including the runway trolley, is 1,065,000 lb. The body length of the vehicle is 219 ft, the wing span is 91 ft, and the height is 33 ft.

From Table 3 it can be seen that while the rocket system accounts for only 8% of the total dry weight, the combined weight of the vehicle structure and the ATR propulsion system accounts for nearly 71%. Therefore, the relative importance of these items in determining overall vehicle characteristics is much greater than for the rocket system and the remaining subsystems.

A weight breakdown of the ascent propellants is as follows. More than 75% of the total propellant by weight is LOX required for the rocket-powered portion of flight, whereas the LOX required for the ATR-powered portion of the flight is only 1.4% of the total. The weight of the LH_2 required for the rocket and ATR modes of flight amount to 12.6 and 10.6% of the total propellant weight, respectively.

Sensitivities

The sensitivity of the reference vehicle dry weight to various parameters used in the weights and sizing analysis is shown in Fig. 12. The sensitivities to structural weight and ATR system weight are the greatest. This is expected, since they are the largest dry weight items. It can be seen from the figure that, if the structural weight factor were 20% greater (representing a 40% weight reduction rather than 50%), the total dry weight would be over 40% greater. The sensitivity of the vehicle to the rocket engine T/W is much lower than the sensitivity of the vehicle to the ATR installed T/W. A 1.0% change in rocket engine T/W results in a 0.2% change in total dry weight, whereas a 1.0% change in ATR installed T/W results in a 1.1% change in total dry weight. Changes of 1% in payload, subsystems, and structural weights result in total dry weight changes of 0.25, 0.65, and 1.75%, respectively. The high sensitivity of the vehicle to weight assumptions illustrates the need for reliable technology forecasts and in-depth analysis if the weights and size are to be accurately predicted.

Conclusions

A single-stage-to-orbit, horizontal-takeoff vehicle concept utilizing ATR and rocket propulsion has been studied. The ATR is used to accelerate the vehicle from takeoff to a speed of Mach 6, after which the vehicle makes a transition to rocket propulsion. The study involved an analysis of vehicle aerodynamics and performance to determine weight and size characteristics assuming the application of advanced technology. Based on the results of this study, the following conclusions were made.

A single-stage-to-orbit vehicle utilizing ATR and rocket propulsion is feasible with advanced technologies, assuming these technologies result in large weight reductions for structures and propulsion. Design features requiring development consist of reusable cryogenic tankage, a launch trolley, thrust vectorable nozzles for the ATR system, variable geometry inlets capable of preventing airflow to the engines, active flight controls, and wing tanks containing liquid oxygen.

The sensitivity of vehicle weight and size to the thrust-to-weight ratio (T/W) at initial conditions and the T/W at rocket start illustrates that optimizing with respect to these parameters is both beneficial and necessary. This is especially true of the initial T/W because of the influence of the ATR system weight-to-thrust ratio, which is much higher than that of the rocket system.

The thrust produced by the ATR in the reference vehicle case is ample for takeoff and acceleration through transonic speeds. The critical region of operation is from Mach 4 to 6. In this region, thrust decreases rapidly, and vehicle performance suffers because of a decreasing thrust-to-drag margin. This indicates that it may be beneficial to make a transition to rocket thrust before Mach 6 or to operate the propulsion systems concurrently before making a transition to rocket power alone.

The heating encountered by the vehicle in the airbreathing phase of flight is relatively benign, based on a comparison of the maximum reference stagnation point heat rates calculated for the airbreathing and rocket-powered flight phases. A substantially higher heat rate is encountered by the vehicle near the end of the rocket-powered phase.

The high sensitivity of the vehicle to weight assumptions, in particular to assumptions on structures and ATR propulsion weights, illustrates the need for reliable technology forecasts and in-depth analysis if the weights and sizes of these vehicle types are to be accurately predicted.

References

[1]Talay, T. A., Stanley, D. O., and Lepsch, R. A., "Advanced Manned Launch System Review," 26th Space Congress, Cocoa Beach, FL, April 1989.

[2]Talay, T. A., and Morris, D. W., "Advanced Manned Launch Systems," AAAF/DGLR/RAES/ESA 2nd European Aerospace Conference, EAC 89-17, Bonn-Bad Godesberg, Germany, May 1989.

[3]Furniss, S. G., "SSTO Design Optimization," 40th Congress of the International Astronautical Federation, IAF-89-222, Malaga, Spain, Oct. 1989.

[4]Luidens, R. W., and Weber, R. J., "An Analysis of Air-Turborocket Engine Performance Including Effects of Component Changes," NACA RM E55HO4a, April 1956.

[5]Hepler, A. K., Zeck, H., Walker, W. H., and Shafer, D. E., "Applicability of the Control Configured Design Approach to Advanced Earth-Orbital Transportation Systems," NASA CR-2723, Aug. 1978.

[6]Freeman, D. C., Jr., and Powell, R. W., "Impact of Far-Aft Center of Gravity for a Single-Stage-to-Orbit Vehicle," *Journal of Spacecraft and Rockets,* Vol. 17, No. 4, 1980, pp. 311-315.

[7]Haefeli, R. C., Littler, E. G., Hurley, J. B., and Winter, M. G., "Technology Requirements for Advanced Earth-Orbital Transportation Systems, Final Report," NASA CR-2866, Oct. 1977.

[8]Ronald, T. F., "Advanced Materials to Fly High in NASP," *Advanced Materials & Processes,* Vol. 135, May 1989, pp. 29-37.

[9]Divan, P. E., "Aerodynamic Analysis System for Conceptual and Preliminary Analysis from Subsonic to Hypersonic Speeds," AIAA Paper 80-1897, Aug. 1980.

[10]Braur, G. L., Cornick, D. E., and Stevenson, R., "Capabilities

and Applications of the Program to Optimize Simulated Trajectories (POST)," NASA CR-2770, Feb. 1987.
[11]Seiden, E. I., Honeycutt, W. D., and Hansen, G. E., "Space Vehicle Weight Estimation Techniques," Convair Aerospace Division, General Dynamics, GDC-ERR-1527-1, San Diego, CA, Dec. 1971.
[12]Anon., "Space Shuttle Synthesis Program (SSSP), Volume II—Weight/Volume Handbook, Final Report," NASA CR-114987, Dec. 1970.
[13]Glatt, C. R., "WAATS—A Computer Program for Weights Analysis of Advanced Transportation Systems," NASA CR-2420, Sept. 1974.
[14]Anon., "Space Shuttle Mass Properties Status Report," Space Division, Rockwell International, SD72-SH-0120-26, Contract NAS9-14000, IRD# SE-482T, WBS-1.2.4.2, Downey, CA, Nov. 2, 1974.
[15]Anon., "Orbiter Detail Weight Statement," Shuttle Orbiter Division, Rockwell International, SD75-SH-0116-124, Contract NAS9-14000, IRD# SE-484EA, WBS 18.3.1.4, Downey, CA, Dec. 2, 1985.
[16]Jackson, L. R., Dixon, S. C., Tenney, D. R., Carter, A. L., and Stephens, J. R., "Hypersonic Structures and Materials: A Progress Report," *Aerospace America,* Vol. 25, No. 10, Oct. 1987. pp. 24–30.

James A. Martin
Associate Editor